Human T-cell leukemia virus type 1 p8 protein increases cellular conduits and virus transmission

Nancy Van Prooyen[a,b], Heather Gold[a], Vibeke Andresen[a], Owen Schwartz[c], Kathryn Jones[d], Frank Ruscetti[e], Stephen Lockett[f], Prabhakar Gudla[g], David Venzon[h], and Genoveffa Franchini[a,1]

[a]Animal Models Retroviral Vaccine Section, Vaccine Branch, National Cancer Institute, National Institutes of Health, Bethesda, MD 20892; [b]Department of Biology, John Hopkins University, Baltimore, MD 21218; [c]Biological Imaging, National Institute of Allergy and Infectious Diseases, National Institutes of Health, Bethesda, MD 20892, [d]Basic Research Program, Science Applications International Corporation–Frederick, National Cancer Institute–Frederick, Frederick, MD 21702; [e]Laboratory of Experimental Immunology, National Cancer Institute–Frederick, Frederick, MD 21702; [f]Optical Microscopy and Analysis Laboratory, National Cancer Institute–Frederick, Frederick MD 21702; [g]Image Analysis Laboratory, Research Tech Program, Science Applications International Corporation–Frederick, National Cancer Institute–Frederick, Frederick, MD 21702; and [h]Biostatistics and Data Management Section, National Cancer Institute, National Institutes of Health, Bethesda, MD 20892

The human T-cell leukemia virus type 1 (HTLV-1) is the cause of adult T-cell leukemia/lymphoma as well as tropical spastic paraparesis/HTLV-1–associated myelopathy. HTLV-1 is transmitted to T cells through the virological synapse and by extracellular viral assemblies. Here, we uncovered an additional mechanism of virus transmission that is regulated by the HTLV-1–encoded p8 protein. We found that the p8 protein, known to anergize T cells, is also able to increase T-cell contact through lymphocyte function-associated antigen-1 clustering. In addition, p8 augments the number and length of cellular conduits among T cells and is transferred to neighboring T cells through these conduits. p8, by establishing a T-cell network, enhances the envelope-dependent transmission of HTLV-1. Thus, the ability of p8 to simultaneously anergize and cluster T cells, together with its induction of cellular conduits, secures virus propagation while avoiding the host's immune surveillance. This work identifies p8 as a viral target for the development of therapeutic strategies that may limit the expansion of infected cells in HTLV-1 carriers and decrease HTLV-1–associated morbidity.

human leukemia retrovirus | orf-I

The human T-cell leukemia virus type 1 (HTLV-1) causes adult T-cell leukemia/lymphoma and tropical spastic paraparesis/HTLV-1–associated myelopathy (1–3). The 3′ end of the viral genome encodes the p12, p8, p13, p30, and HBZ proteins (4–7), whose functions are not fully understood. Here we focused on the function of the p8 protein. Expression of the singly spliced orf-I mRNA yields the endoplasmic reticulum (ER) resident precursor p12 protein. Removal of an ER retention/retrieval signal located at the amino terminus of p12 yields the p8 protein, which traffics to the cell surface (8, 9). The p12 and p8 proteins exert contrasting effects on T cells. The p12 protein induces T-cell activation by increasing ER calcium influx and/or NFAT activity (10). Furthermore, p12 induces T-cell proliferation by binding the IL-2 receptor β and γ chains (11) and by increasing STAT-5 phosphorylation and IL-2 production (12). In contrast, upon T-cell receptor (TCR) ligation, p8 is recruited to the immunological synapse (IS), the contact site between the antigen-presenting cell and the T lymphocytes. Upon T-cell activation, p8 down-regulates proximal TCR signaling and causes T-cell anergy (8, 9). Prior work has demonstrated that, although the orf-I protein products increase T-cell contact by lymphocyte function-associated antigen-1 (LFA-1) clustering (13), they also decrease interaction among T cells by downregulating intercellular adhesion molecule 1 (ICAM-1), ICAM-2, and the MHC-I at the cell surface to avoid recognition by natural killer (NK) cells and cytotoxic T cells (CTL) (14, 15). Here we present data that reconcile these seemingly opposite effects of the p12 and p8 proteins on T cells. We found that p8, but not p12, increases clustering of LFA-1 on the cell surface. In addition, we found that p8 increases the number and length of cel-

lular conduits that enhance communication among several cell types (16–18). Through these conduits, p8 is rapidly transferred to neighboring uninfected T cells, where it augments T-cell contact and HTLV-1 transmission. Thus, HTLV-1 orf-I encodes proteins that increase the proliferation of infected T cells and favor their escape from immune recognition by downregulating MHC-I, ICAM-1, and ICAM-2, and, to the contrary, enhance T-cell contact while anergizing T cells, and induce conduit formation to favor virus transmission.

Results

p8, but Not p12, Protein Increases T-cell Conjugation and HTLV-1 Transmission in T Cells. To dissect the roles of p12 and p8 on HTLV-1 infection of T cells, we constructed cDNA of a natural allele of orf-I that carries a substitution of glycine for serine at position 29. This amino acid change severely impairs cleavage and results in the predominant expression of p12. We also generated a cDNA that encodes p8 (8). We used the HTLV-1 WT molecular clone, pAB, or the p12KO molecular clone deficient in orf-I expression (19). The Jurkat T cells transfected with pAB or p12KO plasmids produced equivalent amounts of virus (19). However, cocultivation with the reporter cell line (BHK1E6) (20), which contains the β-gal gene under the control of the HTLV-1 LTR promoter, revealed that the p12KO virus was significantly less infectious than the WT virus (21) (Fig. 1A, lanes 1 and 2). The p12KO infectivity was rescued by the coexpression of p8, but not p12 (Fig. 1, lanes 3 and 4). The ability of p8 to rescue virus transmission required viral integration and the envelope protein, as demonstrated by the lack of infectivity of the integrase or envelope-defective HTLV-1 molecular clones (22) in the absence or presence of p8 (Fig. 1A, compare lanes 5–7 and 8–10, respectively).

Because p8 traffics to the cell membrane, we hypothesized that p8 may affect cell adhesion. To investigate this, we measured the ability of p8-expressing cells to cluster with each other, by enumerating cell conjugates. The p8, but not the p12, protein significantly increased T-cell conjugates (Fig. 1B) and this effect was actin polymerization-dependent as it was inhibited by cytochalasin D, but not by nocodazole, a tubulin inhibitor (Fig. 1C). The orf-I product(s) has been previously shown to increase LFA-1 clustering (13), suggesting the hypothesis that p8 may increase T-cell contact by clustering LFA-1. p8 expression in Jurkat T cells
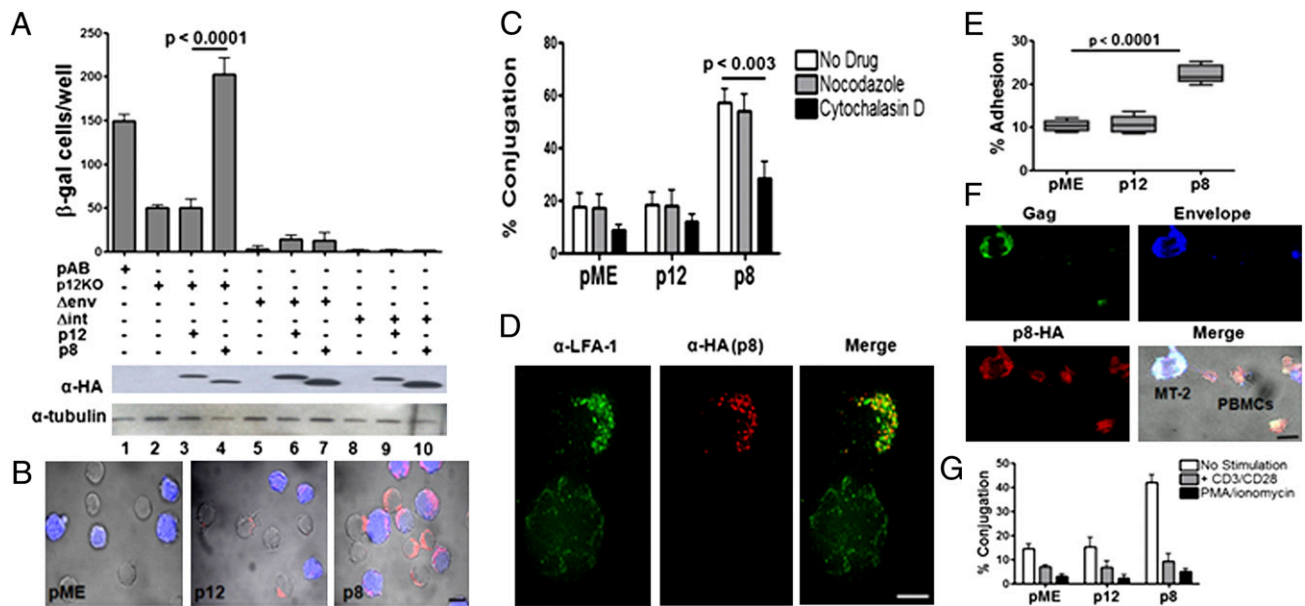
Fig. 1. p8 but not p12 increases T-cell contact and virus transmission. (*A*) Jurkat T cells were transfected with the WT HTLV-1 pAB, p12KO, Δ*env* (defective in the *envelope* gene), or Δ*int* (defective in the *integrase* gene) molecular clones with and without p12 or p8. After 24 h from transfection, the Jurkat T cells were cocultured with the BHK1E6 cells. The data are representative of three independent experiments. Western blots analysis of p12-HA and p8-HA expression and tubulin as control are shown (*Bottom*). (*B*) p8-HA, p12-HA, and control pME transfected Jurkat T cells were mixed at a 1:1 ratio with untransfected Jurkat T cells prestained with CellTracker Orange (blue) for 20 min, fixed, and stained with anti-HA antibody and Alexa-488 (red). (Scale bar, 10 μm.) (*C*) Effects of inhibitors of microtubule (1 μM nocodazole) and actin (1 μM cytochalasin D) on cell conjugation (>300 cells were analyzed and counted per each condition) following transfection of Jurkat T cells with pME, p12-HA, or p8-HA. (*D*) Deconvolution confocal image of one untransfected (bottom cell) and one p8-HA–expressing (red, top cell) Jurkat T cell stained with LFA-1 on the cell surface (green). (Scale bar, 5 μm.) (*E*) Jurkat T cells were plated on ICAM-1 Fc-coated coverslips for 30 min at 37 °C. Adhesion was measured as a percentage of adherent cells of the total cells added per well. Values are mean ± SEM of quadruplicate experiments. MT-2 cells were transfected with pME, p12-HA, or p8-HA expression vectors and mixed at a 1:1 ratio with freshly isolated PBMCs that were in a resting state or stimulated with antibodies toward CD3 and CD28 or PMA/ionomycin (for 24 h), then stained with CellTracker Orange (blue). Cells were stained with anti-HA (red), Gag (green), and Env (blue) and imaged on a confocal microscope. (*F*) An example a single optical section (1 μm) of the formation of a conduit between one MT-2 T cell expressing p8-HA (donor) and two resting PBMCs. (Scale bar, 10 μm.) (*G*) Quantification of the percentage of conduits (a minimum of 40 cells analyzed per conditions) formed among MT-2 and resting or stimulated PBMCs (**P = 0.005).

did not affect LFA-1 surface levels as determined by flow cytometry, but p8 colocalized with clustered LFA-1 (Fig. 1*D*). To address the functional consequence of this finding, we performed an assay using p8- or p12-expressing Jurkat T cells plated on coverslips coated with ICAM-1, the ligand of LFA-1. As demonstrated in Fig. 1*E*, T-cell adhesion was significantly enhanced by p8, but not p12, suggesting that p8 increases T-cell contact, at least in part, through LFA-1. Thus, p8 increases T-cell conjugation through LFA-1 and ICAM-1 interaction, which requires actin and results in an enhancement of virus transmission.

We next assessed whether p8 also increases T-cell contact among primary lymphocytes. As the vast majority of T cells in vivo are in a resting state, we examined both activated and quiescent peripheral blood mononuclear cells (PBMCs). Human PBMCs were purified and stimulated with α-CD3 and α-CD28 antibodies or PMA/ionomycin or left untreated and cultured 24 h with MT-2 cells overexpressing p8 or p12. The Gag, Env, and p8 proteins were visualized in the conduits formed between MT-2 and PBMCs, regardless of their activation status. As an example, one MT-2 cell forms conduits with two resting PBMCs (Fig. 1*F*).We found that conduits were formed between MT-2 and primary T-cell and, interestingly, the percentage of resting T cells that formed conduits with MT-2 cells was significantly higher than that formed by activated T cells (Fig. 1*G*).

p8 Protein Is Rapidly Transferred to T Cells and Augments the Number and Length of Cellular Conduits. Surprisingly, in experiments whereby Jurkat T cells were cocultured with prestained untransfected Jurkat T cells (blue cells), we observed that p8 could be detected in the untransfected neighboring T cell (blue cells; Fig.

2*A*). Quantification of this phenomenon by using fluorescent intensity analysis demonstrated that a significant amount of p8 was transferred to the untransfected prestained Jurkat T cells (Fig. 2*B*). Interestingly, we observed that the surface of p8-expressing T cells had thin membranous conduits (an example is demonstrated in Fig. 2*A*), which are typically found in less than 10% of T cells (16–18). Conduits are membrane structures that contain F-actin, favor cell-to-cell communication, and transport proteins, organelles, and viruses (16–18, 23, 24). To investigate the hypothesis that p8 may increase the conduits' formation, we quantified the number of conduits per cell, as well as the length and curvature of the conduits in p8- or p12-expressing Jurkat T cells (*SI Methods*). p8 expression in Jurkat T cells significantly augmented the percentage of cells with conduits (Fig. 2*C*), the length of the conduits (Fig. 2*D*), and the frequency conduits per cells (Fig. 2*E*). As it is known that the Tax protein, the HTLV-1 transactivator, alone is able to induce polarization of microtubule-organizing center (MTOC) following ICAM-1 engagement (25–27), we investigated whether Tax could influence p8-induced conduit formation. Tax had no effect on conduit length and numbers (Fig. 2 *C*–*E*), suggesting that p8 alone is sufficient to mediate this effect.

The *orf-I* mRNA is expressed at low levels in HTLV-1–infected cells (4, 5), raising the possibility that the ability of p8 to increase cell contact and conduit formation could be an artifact of p8 overexpression, rather than being truly relevant to HTLV-1 infection. To address this hypothesis, we used the p12KO virus that cannot express p8 or p12 (19) and compared it to the WT HTLV-1 for its ability to increase cell contact and conduit formation. The p12KO virus induced significantly less cell conjugates (Fig. 2*F*) and a lower frequency of cells with conduits (Fig. 2*G*), confirming

CELL BIOLOGY

that the expression of the *orf-I* gene during viral replication affects T-cell contact and conduit formation. Importantly, p8, but not p12, restored the ability of the 12KO virus to increase T-cell conjugates and the percentage of T cells with conduits (Fig. 2 *F* and *G*). Thus, the HTLV-1 p8 protein, both in an overexpression system and in the context of a viral infection, increases cell contact and increases the length and number of cellular conduits.

p8 Proteins Increase Virus Transmission, Cell Contact, and Conduit Formation in Naturally Infected T Cells. Next, we wished to test whether p8 enhances virus transmission, cell contact, and conduit formation in T cells naturally infected by HTLV-1. For this purpose, we transfected the MT-2 T-cell line, chronically infected with HTLV-1, with p8- or p12-expressing plasmids and cocultured them with the reporter cell line BHK1E6. We found that MT-2 cells expressing p8 transmitted HTLV-1 significantly better than p12 expressing or mock transfected cells (Fig. 3*A*). Coculture of p8-expressing MT-2 cells, stained for Gag expression (green), with prestained Jurkat T cells (blue), demonstrated that p8, but not p12, significantly increased cell polyconjugates (Fig. 3*B*). Similar to our observation in Jurkat T cells (Fig. 2 *A* and *B*), p8 was also transferred from the MT-2 cells to the prestained untransfected Jurkat T cells (blue; Fig. 3*C*). Importantly, p8-expressing MT-2 cells connected to the prestained Jurkat T cells (blue) through long conduits, and, strikingly, Jurkat T cells that acquired p8 formed conduits as well (Fig. 3*D*). The expression of p8 significantly increased the percentage of MT-2 cells with conduits (Fig. 3*E*) and also the length of the conduits (Fig. 3*F*). The percentage of cells with more than three conduits was higher in p8-expressing MT-2 cells than in p12-expressing or control cells (Fig. 3*G*). There was no significant difference in the average curvature of the conduits among all tested samples ($0.04 \pm 0.01 \ \mu m^{-1}$).

Kinetics of p8-Induced Conduit Formation and Virus Transfer. To investigate the kinetics of conduit formation and virus transmission,

we performed real-time live imaging (*SI Methods*) by using an envelope defective HTLV-1 construct that expresses the Gag protein fused to the YFP (NC-YFP). Previous studies demonstrated that the NC-YFP can be used to visualize HTLV-1 transmission when complemented with the envelope gene (28, 29). MT-2 cells transfected with the NC-YFP and the p8-mCherry plasmids were cocultured with untransfected Jurkat T cells and live images were acquired every 10 s during a 10-min time lapse. A heterogeneous pattern of NC-YFP staining (green), varying from diffuse to bright punctuate signals, was observed at the cell surface similar to fixed images of Gag. In contrast, p8-mCherry (red) was mainly distributed throughout the cell surface and polarized only when in direct cell contact, similar to the p8-HA protein. Infected cells expressing both p8-mCherry and NC-YFP were less mobile compared with cells expressing only NC-YFP alone. Upon encounter with Jurkat T cells, MT-2 cells became less mobile. Frame-by-frame time-lapse analysis of a representative event (Fig. 4*A*) suggested that cellular conduits extended in random directions and toward neighboring Jurkat T cells (Fig. 4*A*). The Gag (green) and p8 (red) proteins were visualized in the conduits and the Gag appeared to reach a neighboring target T cell within a 3-min time span (Fig. 4*A* and Movie S1). During this time span, the cellular conduits extended and retracted, suggesting the high plasticity of these structures. In addition, the formation of conduits was observed after cell-to-cell contact and subsequent cell separation as previously described (16) (Movie S2).

To further characterize virus transfer, we performed transmission EM. Analysis of HTLV-1 p8-expressing MT-2 cells and Jurkat T cells (Fig. 4*B*) demonstrated the presence of viral particles with the characteristic shape of mature HTLV-1, either at the contact sites between two conduits (Fig. 4*C*) or between a conduit and the surface of the target T cell (Fig. 4*D*). Thus, the combined use of live imaging and TEM supports the notion that HTLV-1 can be transmitted upon contact
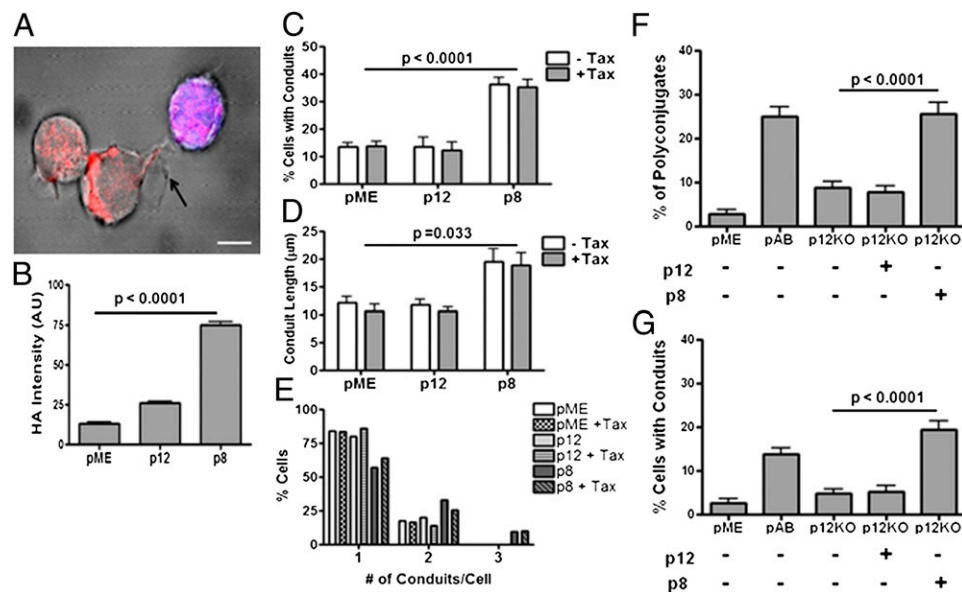

Fig. 2. p8 protein is transferred to T cells and induces cellular conduits. (*A*) p8 (in red) is seen in a neighboring untransfected Jurkat T cell prestained with CellTracker Orange (blue) for 20 min. This picture was obtained 20 min after coculture of expressing and prestained untransfected Jurkat T cells. (Scale bar, 5 μm.) (*B*) Relative mean intensity of HA-staining in prestained untransfected Jurkat T cells (blue) cocultured with p8-HA or p12-HA–expressing (*C–E*) Jurkat T cells (>80 cells counted per condition). Jurkat T cells were left untransfected or transfected with Tax1 with or without p12-HA or p8-HA and mixed with untransfected Jurkat T cells. For each condition, 40 cells were analyzed. We enumerated the percent of cells forming conduits (*C*), the length of each TNT conduit (*D*), and the number of conduits per cell (*E*). Jurkat T cells were cotransfected with the HTLV-1 pAB or the p12KO molecular clones with or without p12 and p8 and mixed with prestained untransfected Jurkat T cells. The percent of cell conjugates (*F*) and the number of cells with conduits (*G*) was calculated on more than 50 cells per condition.
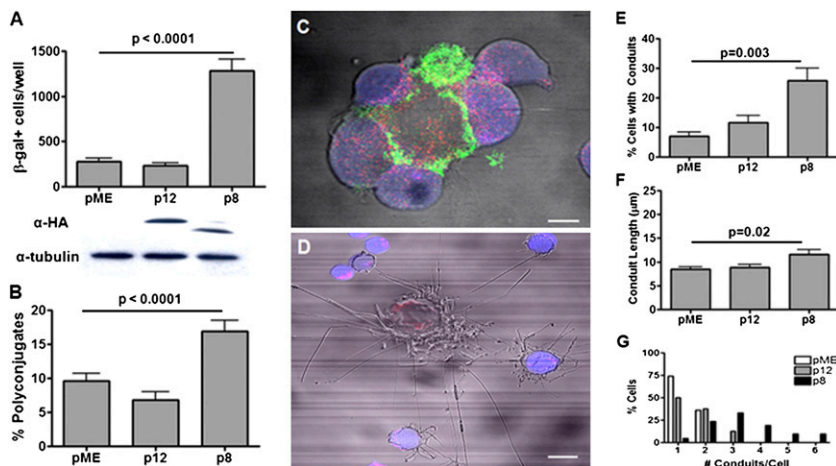
Fig. 3. p8 increases virus transmission from chronically HTLV-1–infected T cells. (*A*) Coculture of MT-2 cells expressing pME, p12, or p8 with the BHK1E6 cells and enumeration of cells expressing β-gal. *Bottom*: Western blot to confirm the expression of p8 and p12 as well as of tubulin as a control. (*B*) MT-2 T cells (donor cells) were transfected with HA-tagged pME, p12, or p8 and mixed at a 1:1 ratio with untransfected prestained Jurkat T cells (blue) and the percentage of cells with conjugates were counted. (*C*) The MT-2 were mixed with Jurkat T cells CellTracker Orange (blue) for 20 min and fixed and stained with anti-HA (red) and anti–HTLV-1 gag (green) antibodies. (Scale bar, 5 μm.) (*D*) The confocal image illustrates a MT-2 cell transfected with p8-HA (red) surrounded by several prestained untransfected Jurkat T cells (blue) and several long cellular conduits. (Scale bar, 10 μm.) (*E*) In the coculture of MT-2 cell and Jurkat T cells, we calculated the percentage of MT-2 cells with conduits, (*F*) the length of conduits, and (*G*) the number of cells containing at least one conduit of 5 μm or longer. The length of each of the conduits was calculated on Fiji Simple Neurite Tracer on more than 50 cells.

with the target cell, not only via the virological synapse, but also through cellular conduits.

Discussion

Transmission of HTLV-1 to T cells and to dendritic cells is more efficient by cell-to-cell contact (30, 31). Upon contact of a target T cell with an HTLV-1–infected T cell, the MTOC reorients toward the cell-to-cell junction (26). The HTLV-1 Gag clusters at the site of cell-to-cell contact, defined as the virological synapse (32). Prolonged contact between an HTLV-1–infected T cell and a target cell is in part because of an increased density of ICAM-1 and LFA-1 molecules at the site of contact (26). Engagement of these molecules is sufficient to trigger the reorientation of the MTOC in HTLV-1–infected T cells toward the cell-to-cell junction (26). Recent work also demonstrates that in both primary and cultured human lymphocytes, HTLV-1 viruses that bud from the cell surface can be
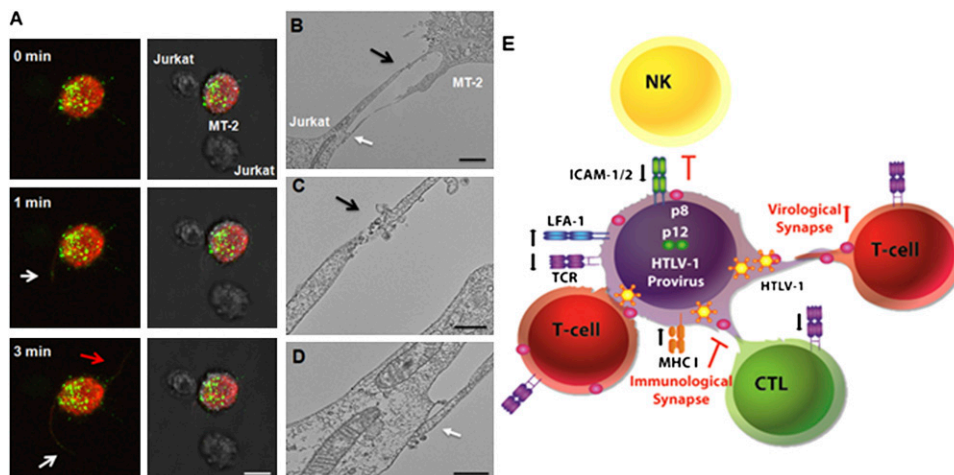
Fig. 4. Kinetics of p8 and virus transfer throughout conduits. (*A*) MT-2 cells were cotransfected with NC-YFP HTLV-1 construct and the p8-mCherry protein (red) and mixed with untransfected Jurkat T cells. Time-lapse microscopy reveals that cellular conduits form within minutes in an MT-2 cell. White arrows indicate transfer of NC-YFP (green) within a cellular conduit to Jurkat T cells. The red arrow indicates the formation of a conduit not directed toward a neighboring T cell. (Scale bar, 10 μm.) (*B–D*) Transmission EM of p8-HA transfected MT-2 T cells mixed with target Jurkat T cells. Virus particles are indicated by a black arrow at the junction between two conduits or by a white arrow at the junction between a conduit and a cell. (*B*) Scale bar, 2 μm. (*C–D*) Scale bar, 500 nm. (*E*) Model of the effect of p12 and p8 on HTLV-1 transmission and immune evasion. An HTLV-1–infected cell (donor), depicted in the center in purple, upon TCR ligation, produces a low level of virus (because p8, by decreasing TCR proximal signaling, decreases NFAT and Tax activity) and escapes immune recognition by CD8+ T cells (CTL in green) and NK cells (in yellow) because the *orf-I* gene down-regulates MHC-I and ICAM-1 and ICAM 2. The expression of p8 in the donor cell increases LFA-1 clustering that in turn recruits T cells (in red). p8-induced conduit formation allows rapid transfer of p8 and virus to all T cells. The newly infected cell will also be anergized by p8. This strategy confers further protection from CTL killing of the donor infected cells, when the newly infected cell is a CTL because the p8-induced down-regulation of TCR will further weaken MHC-I/TCR interaction and inhibit cell killing. This model explains how the perpetuation of this cycle can influence virus persistence in an immune competent host and why HTLV-1–infected individuals have some degree of immune deficiency (46).

entrapped within ECM and linker proteins reminiscent of bacterial biofilms (33). The findings of the current work are not in contradiction with prior data; rather, they demonstrate that HTLV-1 can also be transmitted by cellular conduits. The data presented here, however, reveal that HTLV-I regulates its own transmission by encoding the p8 protein, which, by invading neighboring T cells and by increasing T-cell contact, creates a network of T cells through conduits.

Membrane extensions, such as filopodia bridges, or viral cytonemes, have been shown to be involved in the transmission of several retroviruses (24). Viruses move along the outer surfaces of conduits toward the target cell, appearing as a stretched virological synapse (24, 34). Conduits are thin-membrane extensions, longer than 5 μm, that are believed to be formed by directed outgrowth of a filopodium-like protrusion toward a neighboring cell or by dislodgment after direct cell contact interaction (35–37). In our studies, we did not document "surfing" of HTLV-1 virions on the outside of cellular conduits. Rather, we observed viral particles at the contact site between conduits or between conduits and cells. Thus, HTLV-1 transmission can occur by cell-to-cell contact (38), by adhesion of viral assemblies on the surface of infected cells to uninfected cells, and through cellular conduits, as demonstrated here.

In this work, we have reconciled seemingly contradictory observations of the *orf-I* protein products by dissecting the independent roles of p8 and p12 in cell-to-cell contact and virus transmission. We show that HTLV-1 p8, but not p12, promotes the formation of cell conjugates and conduits between infected T cells and uninfected Jurkat T cells. We observed a similar phenomenon in primary human T cells.

The HTLV-1 p8 protein is an example of convergent evolution among human retroviruses as it targets the same pathways, although by different mechanisms, as the HIV-I Negative regulatory factor (Nef) protein. Both HIV-1 Nef and p8 localize to the IS (8, 39) and both proteins affect the TCR function at the IS (40, 41). Similarly, Herpesvirus saimiri has also been reported to modulate IS function (42). Thus, the modulation of the immune responses at the IS appears to be a conserved evolutionary strategy of viruses that target T and B cells, possibly to safeguard their persistence in immune competent hosts.

The ability of p8 to be transferred to neighboring cells and induce T-cell anergy, while also increasing T-cell contact, represents a unique strategy HTLV-1 has evolved to persist in the host. The Nef protein of HIV is also transferred to B cells to inhibit their function (43). Our hypothesis is that p8 invades neighboring cells to favor rapid transfer of virus, and at the same time, anergizes T cells to protect the infected cells from immune recognition. Thus, p8 complements the ability of *orf-I* to down-regulate MHC-I and ICAM-1 and ICAM-2 expression to protect the infected cells from CTL and NK cells (Fig. 4*E*). This model predicts that virus-specific CTL could be infected by HTLV-1 in vivo. Indeed, Tax-specific CTLs are infected by HTLV-1 with high frequency (44) and CD8$^+$ T cells are a virus reservoir in vivo (45). Furthermore, anergy of HTLV-1–infected T cells in vitro (41) and immune deficiency have been documented in HTLV-1 infection (46). Our finding that p8 is the mediator of these effects provides a unique viral target. The understanding of the mechanisms used by p8 to induce T-cell clustering and conduit formation is of utmost importance as it will guide targeted efforts to limit virus spreading and prevent disease in HTLV-1–infected individuals.

Methods

Cell Culture, Plasmids, and Drug Treatments. MT-2 cells and Jurkat T cells (E6.1) were obtained from American Type Culture Collection and maintained in RPMI media supplemented with 10% FBS, 2 mM L-glutamine, and 100 U/mL antibiotic. MT-2 cells and Jurkat T cells (5 × 10^6) were electroporated (X-05 and H-10, respectively; Amaxa) with 10 μg of DNA plasmid. The HTLV-1 pAB WT, p12KO plasmids, Δ*env* (defective in the *envelope* gene), and Δ*int* (defective in the *integrase* gene) were previously described (9, 28, 29, 19). In the

actin and tubulin remodeling studies, Jurkat T cells were incubated for 1 h at 37 °C with 1 μM nocodazole (Sigma) and 1 μM cytochalasin D (Sigma). The cells were washed three times in PBS solution before mixing with CellTracker orange 541 nm-stained (Invitrogen) target Jurkat T cells. Glass coverslips were coated with 1μg per well of recombinant human ICAM-1/Fc chimera (R&D Systems) in PBS solution in a six-well plate at 4 °C overnight. Nonspecific binding was blocked with 1% BSA in PBS solution for 1 h at room temperature, followed by three washes in PBS solution and one wash in regular media (RPMI medium). Cells (1 × 10^5) were plated on ICAM-1–coated coverslips for 30 min at 37 °C, carefully washed with warm RPMI medium, and fixed. Percentage of attached cells was counted manually. Viral infectivity assays were performed using cocultures of a monolayer of 1 × 10^5 BHK1E6 cells (20), containing a lacZ reporter gene fused to the Tax-responsive promoter HTLV-1 LTR, in a six-well plate with 1 × 10^6 HTLV-1–infected lymphocytes. Monolayers were washed twice with PBS solution 48 h after coculture, fixed with 4% (wt/vol) paraformaldehyde for 15 min, and stained with 200 μg/mL of X-gal solution overnight at 37 °C. Cells were washed twice with PBS solution and β-gal–expressing cells were counted twice, blinded, by bright-field microscopy.

Immunofluorescence. HTLV-1–infected (MT-2) or Jurkat T-cell lines were transfected with pME or p12-HA– or p8-HA–expressing vectors, then mixed 48 h later with target Jurkat T cells prestained with CellTracker Orange 541 nm (Invitrogen). The Jurkat T cells were labeled by incubation with 10 μM CellTracker Orange in OPTI-MEM for 30 min under agitation at 37 °C, then washed twice in regular media. Cells were mixed at a 1:1 ratio on 10 μg/mL fibronectin-coated (Sigma) coverslips and incubated for 1 h at 37 °C. Cells, fixed with 2% paraformaldehyde and 0.1% glutaraldehyde in PBS solution for 2 min at room temperature, were permeabilized with Cytofix-Cytoperm (BD Biosciences) for 5 min at 37 °C and quenched using 50 mM NH$_4$Cl, 20 mM glycine for 5 min at room temperature. Cells were blocked with 2% FBS and 0.2% saponin in PBS solution for 1 h at room temperature, then stained at 37 °C for 1 h with anti-HA (Santa Cruz Biotechnology), anti–HTLV-1 Gag (ZeptoMetrix), or anti–HTLV-1 Env (ZeptoMetrix) antibodies. Quantification of the various cell-to-cell contacts was performed by visual observation of multiple images acquired on a Zeiss 410 LSM confocal microscope with a 63× lens. Cell conjugates were defined as single conjugates and polyconjugates (defined as multiple target cells around a single donor cell).

EM. For transmission EM, HTLV-1–infected donor cells were mixed with target cells at a 1:1 ratio (1 × 10^6 cells in 350 μL). Cells were loaded on fibronectin-coated six-well plates. After 1 h coculture, cells were fixed with 0.1% glutaraldehyde 4% paraformaldehyde in 0.1 M Sorensen buffer (pH 7.2) for 10 min at 37 °C. The samples were processed as previously described (47).

Statistical Analysis. Continuous data that were consistent with normal distributions or could be normalized with logarithmic transformations were compared using one-way ANOVA. For continuous data that could not be made consistent with normality, the exact Wilcoxon rank-sum test was applied in pairwise two-group comparisons. Percentage data that were consistent with a common group mean over samples according to the Fisher–Freeman–Halton test were compared between groups by using a Fisher exact test. Some percentage data were found to be significantly zero-inflated, and a two-parameter model based on the probability of a zero percentage and the group mean of the nonzero samples was assessed by Monte Carlo simulation of Fisher statistic for combining *P* values, conditional on the observed probabilities under the null hypothesis. Count data with small numbers were tested using the exact Cochran–Armitage test for trend. All *P* values are two-tailed and were corrected by the Hochberg method for the three simultaneous tests against the control values appropriate for the comparison.

1. Poiesz BJ, et al. (1980) Detection and isolation of type C retrovirus particles from fresh and cultured lymphocytes of a patient with cutaneous T-cell lymphoma. *Proc Natl Acad Sci USA* 77:7415–7419.
2. Gallo RC (1986) The first human retrovirus. *Sci Am* 255:88–98.
3. Gessain A, et al. (1985) Antibodies to human T-lymphotropic virus type I in patients with tropical spastic paraparesis. *Lancet* 2:407–410.
4. Koralnik IJ, et al. (1992) Protein isoforms encoded by the pX region of human T-cell leukemia/lymphotropic virus type I. *Proc Natl Acad Sci USA* 89:8813–8817.
5. Ciminale V, et al. (1995) Expression and characterization of proteins produced by mRNAs spliced into the X region of the human T-cell leukemia/lymphotropic virus type II. *Virology* 209:445–456.
6. Nicot C, et al. (2004) HTLV-1-encoded p30II is a post-transcriptional negative regulator of viral replication. *Nat Med* 10:197–201.
7. Gaudray G, et al. (2002) The complementary strand of the human T-cell leukemia virus type 1 RNA genome encodes a bZIP transcription factor that down-regulates viral transcription. *J Virol* 76:12813–12822.
8. Fukumoto R, et al. (2009) In vivo genetic mutations define predominant functions of the human T-cell leukemia/lymphoma virus p12I protein. *Blood* 113:3726–3734.
9. Fukumoto R, et al. (2007) Inhibition of T-cell receptor signal transduction and viral expression by the linker for activation of T cells-interacting p12(I) protein of human T-cell leukemia/lymphoma virus type 1. *J Virol* 81:9088–9099.
10. Albrecht B, et al. (2002) Activation of nuclear factor of activated T cells by human T-lymphotropic virus type 1 accessory protein p12(I). *J Virol* 76:3493–3501.
11. Mulloy JC, Crowley RW, Fullen J, Leonard WJ, Franchini G (1996) The human T-cell leukemia/lymphotropic virus type 1 p12I proteins bind the interleukin-2 receptor β and gammac chains and affects their expression on the cell surface. *J Virol* 70:3599–3605.
12. Nicot C, et al. (2001) HTLV-1 p12(I) protein enhances STAT5 activation and decreases the interleukin-2 requirement for proliferation of primary human peripheral blood mononuclear cells. *Blood* 98:823–829.
13. Kim SJ, Nair AM, Fernandez S, Mathes L, Lairmore MD (2006) Enhancement of LFA-1-mediated T cell adhesion by human T lymphotropic virus type 1 p12I1. *J Immunol* 176:5463–5470.
14. Banerjee P, Feuer G, Barker E (2007) Human T-cell leukemia virus type 1 (HTLV-1) p12I down-modulates ICAM-1 and -2 and reduces adherence of natural killer cells, thereby protecting HTLV-1-infected primary CD4+ T cells from autologous natural killer cell-mediated cytotoxicity despite the reduction of major histocompatibility complex class I molecules on infected cells. *J Virol* 81:9707–9717.
15. Johnson JM, et al. (2001) Free major histocompatibility complex class I heavy chain is preferentially targeted for degradation by human T-cell leukemia/lymphotropic virus type 1 p12(I) protein. *J Virol* 75:6086–6094.
16. Sowinski S, et al. (2008) Membrane nanotubes physically connect T cells over long distances presenting a novel route for HIV-1 transmission. *Nat Cell Biol* 10:211–219.
17. Rustom A, Saffrich R, Markovic I, Walther P, Gerdes HH (2004) Nanotubular highways for intercellular organelle transport. *Science* 303:1007–1010.
18. Watkins SC, Salter RD (2005) Functional connectivity between immune cells mediated by tunneling nanotubules. *Immunity* 23:309–318.
19. Valeri V, et al. (2010) Requirement of the human T-cell leukemia virus p12 and p30 genes for infectivity of human dendritic cells and Macaques but not rabbits. *Blood*, 10.1182/blood-2010-05-284141.
20. Astier-Gin T, Portail JP, Lafond F, Guillemain B (1995) Identification of HTLV-I- or HTLV-II-producing cells by cocultivation with BHK-21 cells stably transfected with a LTR-lacZ gene construct. *J Virol Methods* 51:19–29.
21. Taylor JM, et al. (2009) Novel role for interleukin-2 receptor-Jak signaling in retrovirus transmission. *J Virol* 83:11467–11476.
22. Derse D, Hill SA, Lloyd PA, Chung Hk, Morse BA (2001) Examining human T-lymphotropic virus type 1 infection and replication by cell-free infection with recombinant virus vectors. *J Virol* 75:8461–8468.
23. Bukoreshtliev NV, et al. (2009) Selective block of tunneling nanotube (TNT) formation inhibits intercellular organelle transfer between PC12 cells. *FEBS Lett* 583:1481–1488.
24. Sherer NM, Mothes W (2008) Cytonemes and tunneling nanotubes in cell-cell communication and viral pathogenesis. *Trends Cell Biol* 18:414–420.
25. Barnard AL, Igakura T, Tanaka Y, Taylor GP, Bangham CR (2005) Engagement of specific T-cell surface molecules regulates cytoskeletal polarization in HTLV-1-infected lymphocytes. *Blood* 106:988–995.
26. Nejmeddine M, Barnard AL, Tanaka Y, Taylor GP, Bangham CR (2005) Human T-lymphotropic virus, type 1, tax protein triggers microtubule reorientation in the virological synapse. *J Biol Chem* 280:29653–29660.
27. Nejmeddine M, et al. (2009) HTLV-1-Tax and ICAM-1 act on T-cell signal pathways to polarize the microtubule-organizing center at the virological synapse. *Blood* 114:1016–1025.
28. Mazurov D, Heidecker G, Derse D (2006) HTLV-1 Gag protein associates with CD82 tetraspanin microdomains at the plasma membrane. *Virology* 346:194–204.
29. Heidecker G, Lloyd PA, Fox K, Nagashima K, Derse D (2004) Late assembly motifs of human T-cell leukemia virus type 1 and their relative roles in particle release. *J Virol* 78:6636–6648.
30. Ali A, et al. (1993) Dendritic cells infected in vitro with human T cell leukaemia/lymphoma virus type-1 (HTLV-1); enhanced lymphocytic proliferation and tropical spastic paraparesis. *Clin Exp Immunol* 94:32–37.
31. Jones KS, Petrow-Sadowski C, Huang YK, Bertolette DC, Ruscetti FW (2008) Cell-free HTLV-1 infects dendritic cells leading to transmission and transformation of CD4(+) T cells. *Nat Med* 14:429–436.
32. Igakura T, et al. (2003) Spread of HTLV-I between lymphocytes by virus-induced polarization of the cytoskeleton. *Science* 299:1713–1716.
33. Pais-Correia AM, et al. (2010) Biofilm-like extracellular viral assemblies mediate HTLV-1 cell-to-cell transmission at virological synapses. *Nat Med* 16:83–89.
34. Hope TJ (2007) Bridging efficient viral infection. *Nat Cell Biol* 9:243–244.
35. Gerdes HH, Bukoreshtliev NV, Barroso JF (2007) Tunneling nanotubes: A new route for the exchange of components between animal cells. *FEBS Lett* 581:2194–2201.
36. Davis DM, Sowinski S (2008) Membrane nanotubes: Dynamic long-distance connections between animal cells. *Nat Rev Mol Cell Biol* 9:431–436.
37. Rudnicka D, et al. (2009) Simultaneous cell-to-cell transmission of human immunodeficiency virus to multiple targets through polysynapses. *J Virol* 83:6234–6246.
38. Markham PD, Salahuddin SZ, Macchi B, Robert-Guroff M, Gallo RC (1984) Transformation of different phenotypic types of human bone marrow T-lymphocytes by HTLV-1. *Int J Cancer* 33:13–17.
39. Fenard D, et al. (2005) Nef is physically recruited into the immunological synapse and potentiates T cell activation early after TCR engagement. *J Immunol* 175:6050–6057.
40. Thoulouze MI, et al. (2006) Human immunodeficiency virus type-1 infection impairs the formation of the immunological synapse. *Immunity* 24:547–561.
41. Yarchoan R, et al. (1986) Alterations in cytotoxic and helper T cell function after infection of T cell clones with human T cell leukemia virus, type I. *J Clin Invest* 77:1466–1473.
42. Cho NH, et al. (2004) Inhibition of T cell receptor signal transduction by tyrosine kinase-interacting protein of Herpesvirus saimiri. *J Exp Med* 200:681–687.
43. Xu W, et al. (2009) HIV-1 evades virus-specific IgG2 and IgA responses by targeting systemic and intestinal B cells via long-range intercellular conduits. *Nat Immunol* 10:1008–1017.
44. Hanon E, et al. (2000) Fratricide among CD8(+) T lymphocytes naturally infected with human T cell lymphotropic virus type I. *Immunity* 13:657–664.
45. Nagai M, Brennan MB, Sakai JA, Mora CA, Jacobson S (2001) CD8(+) T cells are an in vivo reservoir for human T-cell lymphotropic virus type I. *Blood* 98:1858–1861.
46. Bunn PA, Jr., et al. (1983) Clinical course of retrovirus-associated adult T-cell lymphoma in the United States. *N Engl J Med* 309:257–264.
47. Gonda MA, Aaronson SA, Ellmore N, Zeve VH, Nagashima K (1976) Ultrastructural studies of surface features of human normal and tumor cells in tissue culture by scanning and transmission electron microscopy. *J Natl Cancer Inst* 56:245–263.

CELL BIOLOGY